CONCRETE LIBRARY OF JSCE NO. 14, MARCH 1990

ELASTO-PLASTIC ANALYSIS OF EXPANSIVE BEHAVIOR DUE TO CORROSION OF REINFORCEMENT IN CONCRETE

(Rearrangement in English of paper in Proceedings of JSCE, No.402, Feb. 1989)

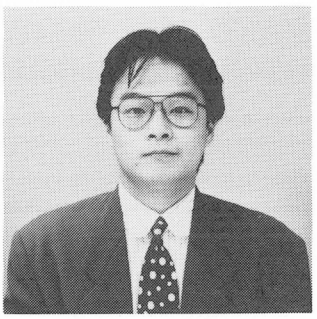

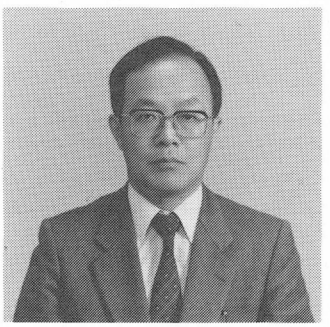

Meguru TSUNOMOTO Yasuo KAJIKAWA Mitsunori KAWAMURA

SYNOPSIS

In order to investigate the expansive behavior and cracking due to the corrosion of reinforcement, the joint element which represents a corroded part was formulated, and the elasto-plastic finite element method with its element which is expanded by introducing the volumetric strain were used in the FEM analysis on a section of RC beams damaged by corrosion.

The analytical results show that the relation between weight-losses of reinforcement and coefficients of expansion for cracking is obtained, and that the pressure and the coefficient of expansion for cracking on a concrete surface is about 10 MPa and 2.0 - 2.2 respectively.

M. Tunomoto is a research engineer at Research and Development Division, Oriental Concrete Co. , Ltd. , Tokyo, Japan. He received his Master of Engineering Degree from Kanazawa University, in 1987. His research interests include analysis of reinforced concrete members by the finite element method, design and dynamic analysis of prestressed concrete bridges. He is a member of JSCE and Japan Prestressed Concrete Engineering Association.

Y. Kajikawa is a professor of Civil Engineering at Kanazawa University, Kanazawa, Japan. He received his Doctor of Engineering Degree from Kyoto University in 1980. His research interests include nonlinear analysis of reinforced concrete members by the finite element method and dynamic analysis of highway bridge. He was awarded a JSCE prize(Tanaka Prize) in 1976 for a series of studies on vibration serviceability of bridge. He is a member of JSCE and JCI.

M. Kawamura is a professor of Civil Engineering at Kanazawa University, Kanazawa, Japan. He received his Doctor of Engineering Degree from Kyoto University in 1971. His research interests include alkali - aggregate reaction, effects of flyash on properties of concrete, micro - structure and fracture of concrete. He was awarded a JCI prize in 1984 and a CAJ prize in 1987 for a series of studies on alkali - silica reaction. He is a member of JSCE, JSMS, JCI, ACI and RILEM.

---

1. INTRODUCTION

Concrete structures have a significant durability among civil engineering structures and have been believed to be maintenance-free ones. In recent years, however, there are some accelerated deterioration problems caused by the corrosion of steel reinforcement and alkali- aggregate reactions in concrete.

Among those problems, there had been many studies[1]-[3] conducted on the problems of the corrosion of reinforcement. Analyses were made for such subject as the mechanism of corrosion, environmental criteria for the corrosion, measures for prevention and un-established on such matters as aging mechanism of whole structure caused by the corrosion of reinforcement, the evaluation of strength , compromised stance on maintenance, and reinforcement to regain that strength.

When reinforcement in concrete is corroded, structural functions of concrete are declined by such phenomena as showed Fig.1, as the decrease of effective area of reinforcement, the destruction of bonding between reinforcement and concrete, the expansive pressure caused by the volume increase (approximately 2 to 4 times) by corrosion and crackings along the direction of reinforcement by the pressure. In recent studies[3]-[6], on the strength of reinforced concrete structures damaged by the corrosion of reinforcement, it was pointed out that the degrees of expansive pressure by the corrosion of reinforcement and transverse cracks caused by the expansive pressure , were determinant parameters related to the strength and the failure modes of reinforced concrete structures. It is, however, very difficult to externally assess the expansive pressure by the corrosion and the condition of cracks which progress within structures. The progress of cracks is influenced by the arrangement of reinforcement and the criteria for expansion so that a lot of works would be required to clarify various situations by experiments.

This study, aims at realizing those behavior analytically by using a finite element method, and assessing the reliability of a model which simulates a behavior of corrosion and expansion relatively well. The model were applied to the investigation of relations between the corrosion of reinforcement in RC beam, and the weight-loss of corrosion and expansive pressure, diameter of reinforcement and cover, tensile strength of concrete, physical characteristics of corrosion products, influences of non-uniform corrosion on expansive behavior. This paper presents the results of those analyses and the method of study on crack condition and the stress distributions within structures. They are considered to provide an important suggestion toward further study on the estimation of strength and the maintenance of structures damaged by the corrosion of reinforcement.

2. MODEL FOR EXPANSIVE BEHAVIOR BY CORROSION

There are following two methods to analytically realize an expansive behavior by corrosion of reinforcement;

(1) the method in which an expansive pressure is applied internally as a force around the reinforcement.

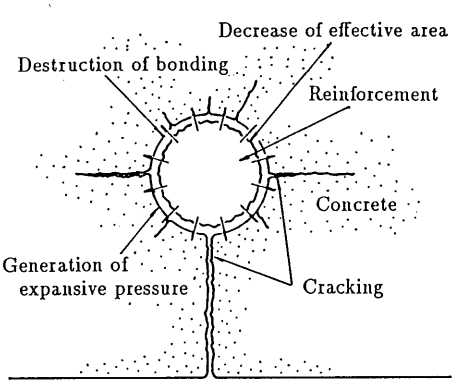

Fig.1 Damaged factors by corrosion of reinforcement

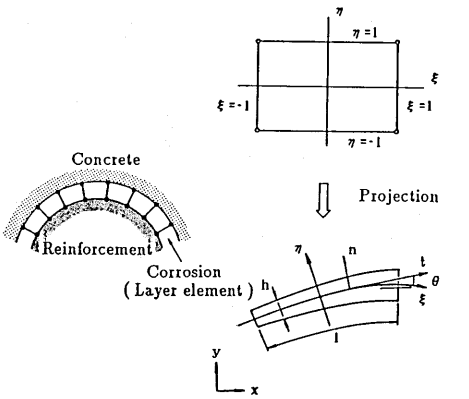

Fig.2 Model of corrosion by layer element

(2) the method in which a volumetric strain is applied as expansion of a model of a corroded layer.

Method (1) can be handled simpler than method (2). This method, however, sometimes give un-realistic results analytically depending on the models for analysis (for example, when there is an angled corner such as shown in Fig.6); causing producing cracks from the surface of concrete and also becoming difficult to converge after crackings. Value of expansive pressure at cracking could be analyzed, though, relations among the weight-losses of corrosion are not clear and the method often gives un-realistic results. From those points of view, the method (2) is considered to present practically similar expansive behavior by corrosion.

In the discussion of corrosion problems of reinforcement in concrete, objective range of weight-loss of corrosion is approximately between 10^{-3} and 10^{-1} g/cm^2. This is equal to a very thin thickness of corrosion between 10^{-3} and 10^{-1} mm. When the method (2) is used, therefore, the element modeling a corrosion products layer is very thin, and high in aspect ratio. There could be many inconveniences in numerical calculations when using normal elements. In this analysis, as to the elements derived from joint elements suggested by Yamada, et al.[7], was adopted.

2.1 Formulation for Layer Element

Concept of layer element is shown in Fig.2, and its formulation is presented hereunder.

Following relation is valid for displacement increment $\dot{u}_t, \dot{u}_n$(hereinafter referred to as $\dot{u}_L$) at the local coordinates t-n.

$$\left\{ \begin{array}{c} \frac{\partial \dot{u}_L}{\partial \xi} \\ \frac{\partial \dot{u}_L}{\partial \eta} \end{array} \right\} = \left[\begin{array}{cc} \frac{\partial t}{\partial \xi} & \frac{\partial n}{\partial \xi} \\ \frac{\partial t}{\partial \eta} & \frac{\partial n}{\partial \eta} \end{array} \right] \left\{ \begin{array}{c} \frac{\partial \dot{u}_L}{\partial t} \\ \frac{\partial \dot{u}_L}{\partial n} \end{array} \right\} \tag{1}$$

When a rule of projection for geometric shape of element at global coordinates x-y is also presented as;

$$\left. \begin{array}{l} x = x(\xi, \eta) \\ y = y(\xi, \eta) \end{array} \right\} \tag{2}$$

Eq.(1) is presented as the following.

$$\left\{ \begin{array}{c} \frac{\partial \dot{u}_l}{\partial \xi} \\ \frac{\partial \dot{u}_l}{\partial \eta} \end{array} \right\} = \left[\begin{array}{cc} \frac{l_2}{2} & 0 \\ \frac{l_3}{2} & \frac{h}{2} \end{array} \right] \left\{ \begin{array}{c} \frac{\partial \dot{u}_l}{\partial t} \\ \frac{\partial u_l}{\partial n} \end{array} \right\} \tag{3}$$

Where;

$$l_2 = 2\sqrt{\left(\frac{\partial x}{\partial \xi}\right)^2 + \left(\frac{\partial y}{\partial \xi}\right)^2} \tag{4}$$

$$\left. \begin{array}{ll} l_3 = 2\sqrt{\left(\frac{\partial x}{\partial \eta}\right)^2 + \left(\frac{\partial y}{\partial \eta}\right)^2} & \left(\frac{\partial t}{\partial \eta} \geq 0\right) \\ l_3 = -2\sqrt{\left(\frac{\partial x}{\partial \eta}\right)^2 + \left(\frac{\partial y}{\partial \eta}\right)^2} & \left(\frac{\partial t}{\partial \eta} \leq 0\right) \end{array} \right\} \tag{5}$$

$$h = \frac{2\left\{\left(\frac{\partial x}{\partial \xi}\right)\left(\frac{\partial y}{\partial \eta}\right) - \left(\frac{\partial y}{\partial \xi}\right)\left(\frac{\partial x}{\partial \eta}\right)\right\}}{\sqrt{\left(\frac{\partial x}{\partial \xi}\right)^2 + \left(\frac{\partial y}{\partial \xi}\right)^2}} \tag{6}$$

Further, when $\partial t/\partial \xi$ is constant then $l_2 = l$, and when nodes which are facing each other have same coordinates then $l_3 = 0$.

Inverse transformation of Eq.(3) is;

$$\left\{ \begin{array}{c} \frac{\partial \dot{u}_l}{\partial t} \\ \frac{\partial \dot{u}_l}{\partial \eta} \end{array} \right\} = \frac{2}{h l_2} \left[\begin{array}{cc} h & 0 \\ -l_3 & l_2 \end{array} \right] \left\{ \begin{array}{c} \frac{\partial \dot{u}_l}{\partial \xi} \\ \frac{\partial \dot{u}_l}{\partial \eta} \end{array} \right\} \tag{7}$$

The transformation rule of coordinates between local and global coordinates is;

$$\left\{\frac{\partial \dot{u}_L}{\partial \xi}\right\} = \left\{\begin{array}{c} \frac{\partial \dot{u}_t}{\partial \xi} \\ \frac{\partial \dot{u}_n}{\partial \xi} \end{array}\right\} = \left[\begin{array}{cc} \cos\theta & \sin\theta \\ -\sin\theta & \cos\theta \end{array}\right] \left\{\begin{array}{c} \frac{\partial \dot{u}_x}{\partial \xi} \\ \frac{\partial \dot{u}_y}{\partial \xi} \end{array}\right\} = [\boldsymbol{T}] \left\{\frac{\partial \dot{u}_G}{\partial \xi}\right\} \tag{8}$$

$$\left\{\frac{\partial \dot{u}_L}{\partial \eta}\right\} = [\boldsymbol{T}] \left\{\frac{\partial \dot{u}_G}{\partial \eta}\right\} \tag{9}$$

Where, $\dot{u}_G$ is a displacement increment at global coordinates. θ is an angle between axis t and x and represented by the following equation.

$$\left.\begin{array}{l} \cos\theta = \dfrac{\frac{\partial x}{\partial \xi}}{\sqrt{\left(\frac{\partial x}{\partial \xi}\right)^2 + \left(\frac{\partial y}{\partial \xi}\right)^2}} \\ \sin\theta = \dfrac{\frac{\partial y}{\partial \xi}}{\sqrt{\left(\frac{\partial x}{\partial \xi}\right)^2 + \left(\frac{\partial y}{\partial \xi}\right)^2}} \end{array}\right\} \tag{10}$$

It shall be presented as follows that displacement velocity $\dot{u}_G$ at global coordinates introduces shape function $N_i(\xi, \eta)$ and uses node velocity $\dot{u}_{Gi}$.

$$\dot{u}_G = \sum_i N_i(\xi, \eta) \dot{u}_{Gi} \tag{11}$$

And then, each grade of displacement velocity becomes as follows;

$$\left\{\begin{array}{c} \frac{\partial \dot{u}_G}{\partial \xi} \\ \frac{\partial \dot{u}_G}{\partial \eta} \end{array}\right\} = \left[\begin{array}{cccc} \frac{\partial N_1}{\partial \xi} & \frac{\partial N_2}{\partial \xi} & \cdots & \frac{\partial N_m}{\partial \xi} \\ \frac{\partial N_1}{\partial \eta} & \frac{\partial N_2}{\partial \eta} & \cdots & \frac{\partial N_m}{\partial \eta} \end{array}\right] \left\{\begin{array}{c} \dot{u}_{G1} \\ \dot{u}_{G2} \\ \cdots \\ \dot{u}_{Gm} \end{array}\right\} \tag{12}$$

In the reference[7], a grade of velocity for only a direction n for joint element is considered. In this study however, a grade of velocity for a direction t shall be considered in order to provide volumetric expansion and together with Eq.(7) to (9);

$$\left\{\begin{array}{c} \frac{\partial \dot{u}_t}{\partial t} \\ \frac{\partial \dot{u}_n}{\partial t} \\ \frac{\partial \dot{u}_t}{\partial n} \\ \frac{\partial \dot{u}_n}{\partial n} \end{array}\right\} = \frac{2}{hl_2} \left[\begin{array}{cccc} h\cos\theta & h\sin\theta & 0 & 0 \\ -h\sin\theta & h\cos\theta & 0 & 0 \\ -l_3\cos\theta & -l_3\sin\theta & l_2\cos\theta & l_2\sin\theta \\ l_3\sin\theta & -l_3\cos\theta & -l_2\sin\theta & l_2\cos\theta \end{array}\right] \left\{\begin{array}{c} \frac{\partial \dot{u}_x}{\partial \xi} \\ \frac{\partial \dot{u}_y}{\partial \xi} \\ \frac{\partial \dot{u}_x}{\partial \eta} \\ \frac{\partial \dot{u}_y}{\partial \eta} \end{array}\right\} \tag{13}$$

Also, strain vector can be presented by the following.

$$\varepsilon = \left\{\begin{array}{c} \varepsilon_t \\ \varepsilon_n \\ \gamma_{tn} \end{array}\right\} = \left\{\begin{array}{c} \frac{\partial \dot{u}_t}{\partial t} \\ \frac{\partial \dot{u}_n}{\partial n} \\ \frac{\partial \dot{u}_t}{\partial n} + \frac{\partial \dot{u}_n}{\partial t} \end{array}\right\} \tag{14}$$

Hence, the relation between displacement and strain in the layer element is given by Eq.(12) to (14);

$$\varepsilon = \left\{\begin{array}{c} \varepsilon_t \\ \varepsilon_n \\ \gamma_{tn} \end{array}\right\} = \frac{2}{hl_2} \left[\begin{array}{cc} h\cos\theta\frac{\partial N_i}{\partial \xi} & h\sin\theta\frac{\partial N_i}{\partial \xi} \\ l_3\sin\theta\frac{\partial N_i}{\partial \xi} - l_2\sin\theta\frac{\partial N_i}{\partial \eta} & -l_3\cos\theta\frac{\partial N_i}{\partial \xi} + l_2\cos\theta\frac{\partial N_i}{\partial \eta} \\ (l_3\cos\theta - h\sin\theta)\frac{\partial N_i}{\partial \xi} + l_2\cos\theta\frac{\partial N_i}{\partial \eta} & \\ (l_3\sin\theta + h\cos\theta)\frac{\partial N_i}{\partial \xi} + l_2\sin\theta\frac{\partial N_i}{\partial \eta} & \end{array}\right] \{u_i\} = [\boldsymbol{B}]\{u_i\} \tag{15}$$

Constitutive rule of element modeling corrosion products can be used the same of plain strain analysis;

$$\{\sigma\} = \left\{\begin{array}{c} \sigma_t \\ \sigma_n \\ \tau_{tn} \end{array}\right\} = \frac{E}{(1+\nu)(1-2\nu)} \left[\begin{array}{ccc} 1-\nu & \nu & 0 \\ \nu & 1-\nu & 0 \\ 0 & 0 & \frac{1-2\nu}{2} \end{array}\right] \left\{\begin{array}{c} \varepsilon_t \\ \varepsilon_n \\ \gamma_{tn} \end{array}\right\} = [\boldsymbol{D}]\{\varepsilon\} \tag{16}$$

A stiffness matrix $\boldsymbol{K}$ of layer element at the global coordinates presents as follows;

$$\boldsymbol{K} = \int_{-1}^{+1}\int_{-1}^{+1} [\boldsymbol{B}]^T[\boldsymbol{D}][\boldsymbol{B}]|\boldsymbol{J}'|sd\xi d\eta \tag{17}$$

Where, $|\boldsymbol{J}'| = hl_2/2$ and s is a thickness of element.

2.2 Expansion Model

Expansive behavior by corrosion was modeled by providing a virtual strain in elements and the expansion force was represented by a consistent nodal force to the element which is considered as virtual load. Since an expansion of corrosion is a volume change, shear strain does not exist. Therefore, in plain strain analysis, when the coefficient of a linear expansion is $d\varepsilon_v$ then the virtual strain $d\varepsilon_o$ becomes as follows;

$$d\varepsilon_o = \begin{Bmatrix} d\varepsilon_t \\ d\varepsilon_n \\ d\gamma_t n \end{Bmatrix} = \begin{Bmatrix} (1+\nu)d\varepsilon_v \\ (1+\nu)d\varepsilon_v \\ 0 \end{Bmatrix} \tag{18}$$

Initial stress in elements by this virtual strain is;

$$d\sigma_0 = -[\boldsymbol{D}]d\varepsilon_0 \tag{19}$$

$$d\sigma_z = -Ed\varepsilon_v \tag{20}$$

The consistent nodal force $\{d\boldsymbol{F}\}$ is presended as follows;

$$\{d\boldsymbol{F}\} = -\int_\Omega [\boldsymbol{B}]^T d\sigma_0 d\Omega \tag{21}$$

3. METHOD FOR NON-LINEAR ANALYSIS OF RC STRUCTURE

There are concrete and reinforcement as structural material surrounding product of reinforcement corrosion. Reinforcement keeps linear characteristics until high stress level though, concrete ends up in cracks and non-linear deformation at low stress level, resulting in complex behavior as a whole structure. Concrete model adopted in this study is presented hereafter[8][9].

3.1 Non-linear Characteristics of Concrete

In this study, a plastic theory model given by associated flow rule and isotropic strain hardening rule was adopted as a non-linear stress-strain relation of concrete. Eq.(22) represent elasto-plastic constitutive rule obtained from plastic theory.

$$\{d\sigma\} = \left([\boldsymbol{D}] - \frac{[\boldsymbol{D}]\left\{\frac{\partial f}{\partial \sigma}\right\}\left\{\frac{\partial f}{\partial \sigma}\right\}^T[\boldsymbol{D}]}{A + \left\{\frac{\partial f}{\partial \sigma}\right\}^T[\boldsymbol{D}]\left\{\frac{\partial f}{\partial \sigma}\right\}} \right) \{d\varepsilon\} \tag{22}$$

Where, $\{d\sigma\}$ is incremental stress vector, $\{d\varepsilon\}$ is incremental strain vector, $[\boldsymbol{D}]$ is elastic constitutive matrix and f is yield function.

Also;

$$A = 2\tau \frac{d\tau}{d\bar{\varepsilon}_p} \sqrt{\left\{\frac{\partial f}{\partial \sigma}\right\}^T \left\{\frac{\partial f}{\partial \sigma}\right\}} \tag{23}$$

$$\bar{\varepsilon}_p = \int d\varepsilon_p = \int \sqrt{d\varepsilon_{ij}^p d\varepsilon_{ij}^p} \tag{24}$$

Where, τ and ε_p are equivalent stress and plastic strain respectively.

Further, yield function f was adopted the same function as failure criterion of concrete which is presented later on.

3.2 Failure Criterion

As to the failure criterion, a combined one of tension - cutoff and Drucker - Prager criterion was adopted which is represented by Eq.(25).

$$f(I_1, J_2) = \alpha I_1 + \sqrt{J_2} - k' = 0 \tag{25}$$

Where, I_1 and J_2 are the first invariant of stress tensor and the second invariant of stress deviator tensor respectively. α, k are parameters to determine failure criterion. They are set, referring to experimental results of Kupfer et al.[10], to mach uniaxial failure strength f_c and equivalent biaxial failure strength $f_{bc} = 1.16 f_c$ and adopted as $\alpha = 0.07$, $k' = 0.507 f_c$. Fig.3 shows failure criterion adopted to the analysis.

As to the mode of failure, when Eq.(26) is valid there is a crushing failure, and otherwise there is a cracking.

$$\sqrt{J_2} \leq -1/3 \cdot I_1 \qquad \text{and} \qquad I_1 \leq 0 \tag{26}$$

3.3 Cracking Model

For a cracking model, smeared - cracking model was used for that easy application. Constitutive rule after cracking is presented by Eq.(27).

$$\begin{Bmatrix} d\sigma_t \\ d\sigma_n \\ d\tau_{tn} \end{Bmatrix} = \begin{bmatrix} 0 & 0 & 0 \\ 0 & \frac{E}{(1-\nu^2)} & 0 \\ 0 & 0 & \beta G \end{bmatrix} \begin{Bmatrix} d\varepsilon_t \\ d\varepsilon_n \\ d\gamma_{tn} \end{Bmatrix} \tag{27}$$

Where, n and t represent directions of principal stress as shown in Fig.4. Also, shear modulus βG, which represents the aggregate interlocking at the cracked plane, was defined by Eq.(28) while referring by Aoyagi et al.[11].

$$\beta G = G\varepsilon_0/\varepsilon \tag{28}$$

Where, ε is a normal strain to the crack and ε_0 is a strain at the time of cracking.

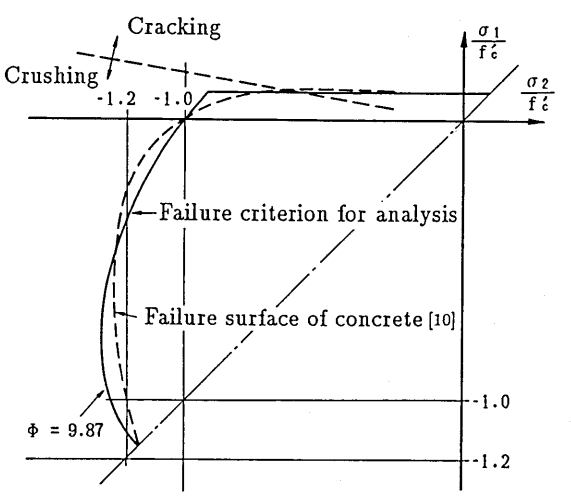

Fig.3 Failure criterion of concrete

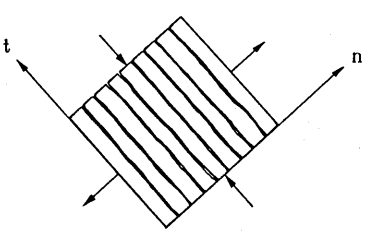

Fig.4 Smeared cracking model

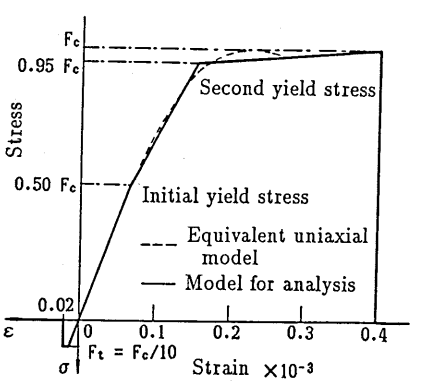

Fig.5 Uniaxial stress - strain relation of concrete for analysis

3.4 Uniaxial Stress-strain Relation of Concrete

Fig.5 shows uniaxial stress-strain relation of concrete adopted for analyses. Tensile side becomes perfectly plastic when a maximum principal stress reaches tensile strength, and a crack shall occur when the principal tensile strain reaches 200 μ.

3.5 Joint Element of Reinforcement and Concrete

At the surface in between reinforcement and concrete, joint element suggested by Yamada et. al.[7] was adopted. That is, constitutive rule is presented by the following equation.

$$\begin{Bmatrix} \dot{\sigma}_{tt} \\ \dot{\sigma}_{tn} \end{Bmatrix} = \begin{Bmatrix} G_E & 0 \\ 0 & G_S \end{Bmatrix} \begin{Bmatrix} \frac{\partial \dot{u}_t}{\partial t} \\ \frac{\partial \dot{u}_n}{\partial n} \end{Bmatrix} = [D] \begin{Bmatrix} \varepsilon \\ \gamma \end{Bmatrix} \tag{29}$$

This element was handled as a part of concrete and after failure, the joint element was handled as $G_S = 0$ when σ is in compression and as $G_S = 0$ and $G_E = 0$ when σ is in tension.

3.6 Layer Element Representing Corrosion Product

Layer element, as mentioned above, was put on a surface of reinforcement by a width of h as shown by Eq.(30), depending on an objective weight-loss of corrosion.

$$h = \frac{\Delta w}{\rho} \tag{30}$$

Where, h ; width of layer element representing corrosion product (cm)

Δw ; weight-loss of corrosion (g/cm^3)

ρ ; density of steel (7.85 g/cm^3)

Eq.(31) was increased incrementally toward the weight-loss of corrosion.

$$\mathrm{d}V = (1 + \mathrm{d}\varepsilon_v)^3 \tag{31}$$

where, $\mathrm{d}V$ is the coefficient of volume expansion and $d_{\varepsilon V}$ is the virtual strain shown in Eq.(19).

4. CALCULATION AND ANALYSIS OF EXPANSIVE BEHAVIOR BY CORROSION

This study adopted an iso-parametric element (8-node serendipity quadrilateral element) and analyzed expansive behavior as a plain strain problem.

Fig.6 and Fig.7 shows the models of reinforced concrete in this study. Among those, a model shown in Fig.6 (hereinafter referred to as model A) has at the middle of square concrete, the layer element representing a corrosion products layer and reinforcement with 0.1 mm wide bond element between them. By the model A (Fig.6), expansive pressure was sought, while analyzing for different parameters such as diameter and cover, uniaxial tensile strength of concrete, elastic modulus of corrosion products and poisson's ratio.

In the case of symmetric model such as model A, when the width of layer element is the same all round, tensile stresses of tangent direction at diagonal position surpasses others due to the differences of deformation between up-down and right-left direction and diagonal direction, and then cracks towards diagonal direction develop resulting in un-real behavior. Therefore, since the weight loss of corrosion in actual situation is not the same all around, each width of layer element representing corrosion products for model A was set normal at random in between 0 and twice of the average width.

The model shown in Fig.7 (hereinafter referred to as model B) was modeled after a section of beam. There are two reinforcements with the diameter of 16 mm with the cover of 30 mm from bottom and

40 mm from sides with the rectangular section, of 150 by 200 mm. Using this model B, cracking situation of beam sample was analyzed by varying width of layer element at the top and bottom of reinforcement which represents the difference of condition of corrosion caused by the casting direction, the condition of cure and the arrangement of testing material at the time of corrosion tests.

4.1 Examples of Calculations

Fig.8 shows examples of calculation for the model A. In this case, the conditions of calculations were; diameter of reinforcement was 25 mm; the cover was 70 mm; the uniaxial tensile strength was 3.5 MPa; the elastic modulus of corrosion products was 200 MPa and Poisson's ratio was 0.3. Then Fig.8 presents the condition of cracking for each coefficient of expansion at weight-loss of corrosion of 10 mg/cm^2. In this example, when the coefficient was 2.2, then cracking reached concrete surface. Time of cracking was determined to be at the strain of 200 μ on the surface.

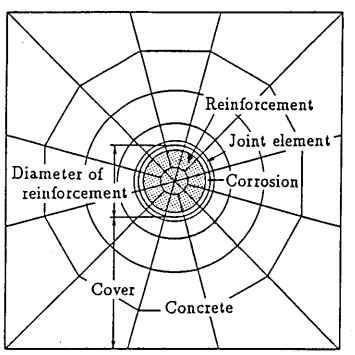

Fig.6 Finite-element model (model A)

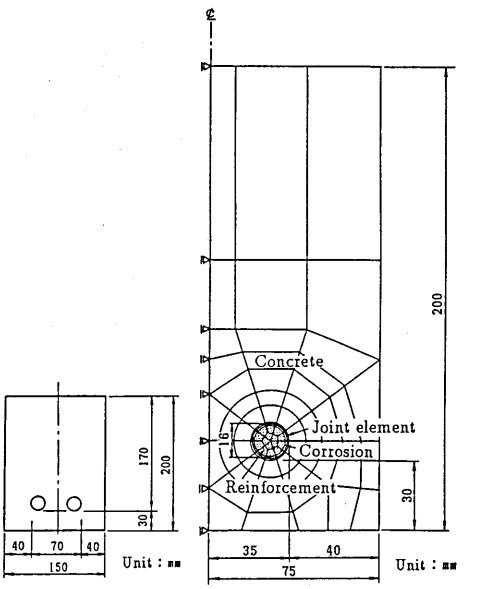

Fig.7 Finite-element model (model B)

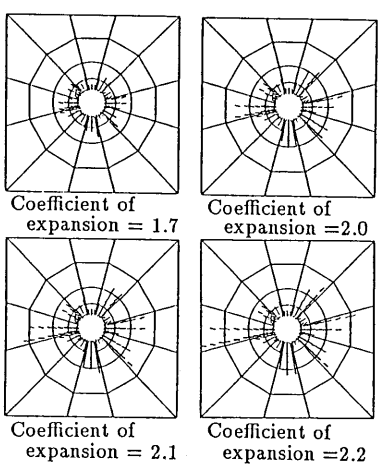

Fig.8 Crack situation for coefficients of expansion

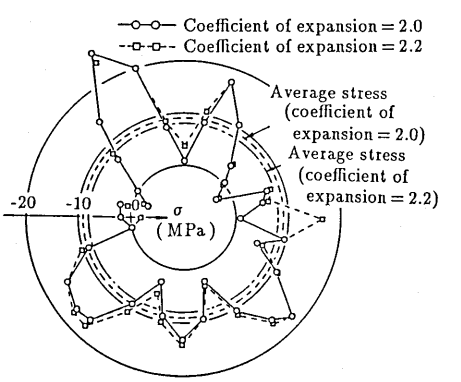

Fig.9 Concrete stress distribution

4.2 Estimation of Expansive Pressure by Corrosion

It is important to estimate expansive pressure by corrosion so as to know stress situation and cracks within concrete. Expansive pressure was obtained, therefore, using this analysis.

In this analysis, since there occurs shear deformation in layer elements by non-uniform deformation after crackings inside of elements, expansive pressure can not be understood as hydrostatic pressure working inside of layer elements. Expansive pressure therefore was evaluated as constrain stress around the surface of reinforcement. Fig.9 show, normal stress distribution of concrete at 0.6 mm point from the surface of reinforcement, in situation of coefficient of expansion to be 2.0 (right before surface cracking) and 2.2 (after surface cracking)in Fig.8. Though there are deviation at some points due to stress release after cracking inside of concrete, there is not large difference of stress between right before and after cracking. Average stresses were approximately 9-10 MPa. According to the experiment by Seki et al.[12] the weight-loss of corrosion for cracking was approximately 10 mg/cm^2 when there was chleride added to concrete. The expansive pressure, therefore, was approximately 9-10 MPa for cracking and coefficient of expansion was considered to be somewhere between 2.0 and 2.2.

4.3 Influence of Elastic Modulus and Poisson's Ratio of Corrosion Product

It is suggested by the reference[13] that the physical characteristics of corrosion product varies according to its binding condition. Therefore, by focusing on elastic modulus and Poisson's ratio as representing physical characteristics of corrosion products, their influences on expansive behavior by corrosion was investigated. Using the analytical results for the model A, Fig.10 shows the relation between weight-loss of corrosion and coefficient of expansion for cracking utilizing elastic modulus of corrosion product as a parameter. The curve in the figure shows a regression when the relation between the weight-loss of corrosion and coefficient of expansion was assumed to be in inverse proportion. According to the result shown in Fig.10, the weight-loss of corrosion for cracking does not depend on the elastic modulus. Yoshioka et al.[13] suggested that the elastic modulus of corrosion products after an accelelated galvanostatic corrosion method was between 200-300 MPa under constraint conditions and 20-50 MPa under unconstraint condition. The result shown in Fig.10 suggests that there is no practical difference by the elastic modulus of corrosion products and it has become clear that the elastic modulus of corrosion products does not much influence for the cracking.

Fig.11 also shows a relation between weight-loss of corrosion and coefficient of expansion for cracking when Poisson's ratio were 0.2 and 0.3. Other criteria were the same as those for Fig.10. According to the results shown in Fig.11, the coefficient of expansion for cracking is influenced somewhat by the Poisson's ratio of corrosion product. Difference, however is small and it was made clear that the Poisson's ratio does not, just the same as the elastic modulus, influence cracking.

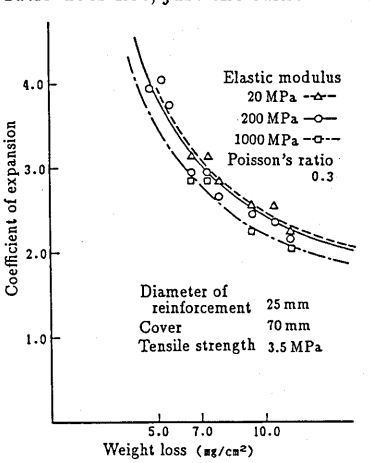

Fig.10 Influence of elastic modulus of corrosion products

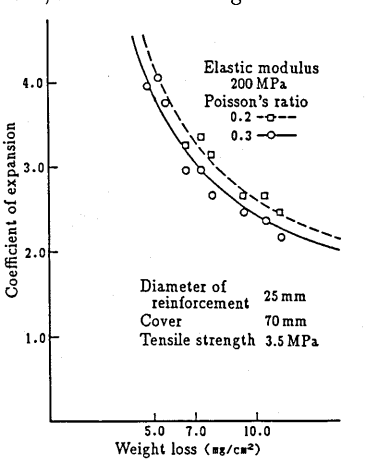

Fig.11 Influence of Poisson's ratio of corrosion products

4.4 Influence of Cover and Tensile Strength of Concrete

Cover and tensile strength of concrete are considered to be factors influencing for cracking . Its influence, therefore, was investigated using this analysis.

Fig.12 shows, the relation between the cover and the weight-loss of corrosion for cracking in the analysis for the model A. In this instance, the diameter of reinforcement was 25 mm, tensile strength of concrete was 3.5 MPa and the Poisson's ratio and elastic modulus of corrosion products were 0.3 and 200 MPa, respectively. Comparing with the result of experiment[12], the result of analysis shows a good consistency with the results of experiment, and it was found by this analysis that the cover influences greatly for cracking.

Fig.13 shows, the relation between the tensile strength of concrete and the weight-loss of corrosion for cracking. In this instance, the diameter of reinforcement was 25 mm, the cover was 70 mm, Poisson's ratio and elastic modulus of corrosion product were 0.3 and 200 MPa, respectively. Uniaxial tensile strength of concrete was assumed to be 2.5-4 MPa, referring to the experiments conducted by Seki et al.[12]. In the Fig. 13, the weight-loss of corrosion for cracking was tried to obtain in relation to the assumed coefficient of expansion and uniaxial tensile strength of concrete. It was considered in general that the weight-loss of corrosion for cracking was larger in parallel with higher uniaxial tensile strength of concrete. Experiments by the reference[12], however, suggested that it does not have as much practical influence as that of the cover. It was also found by this analysis that the influence of tensile strength of concrete was very small comparing to that of the cover.

4.5 Influence of Non-Uniform Corrosion on Crack Situation

Actualy, the extent of corrosion at the top and bottom of reinforcement is different in each other due to bleeding and similar other matters, and the corrosion at the bottom tends to be greater. Using the model B (Fig.7) therefore, the crack situation was investigated in relation to the extent of corrosion which was represented by introducing different ratio of weight-loss of corrosion between the top and the bottom of reinforcement while keeping the total weight-loss of corrosion. Fig.14 shows the result. Inclination of side cracking from level was approximately 60 degrees when the ratio of weight-loss between the top and the bottom was 1 : 1 and approximately 30 degrees for 1 : 5. As shown in Fig.15, cracks toward the side observed during experiment[14][15] had 20-40 degrees inclination from level. It was found also in this analysis that the situation of cracks could rather be understood by considering the difference of extent of corrosion between the top and the bottom.

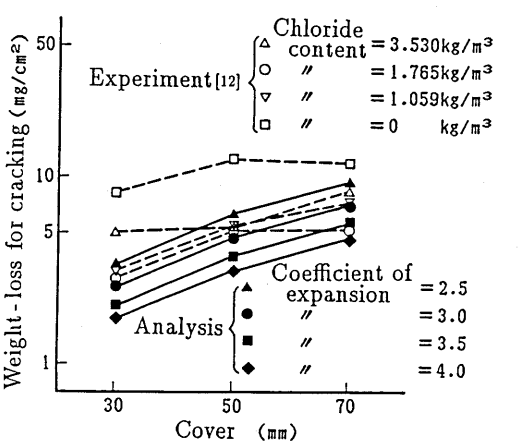

Fig.12 Cover vs. weight-loss for cracking

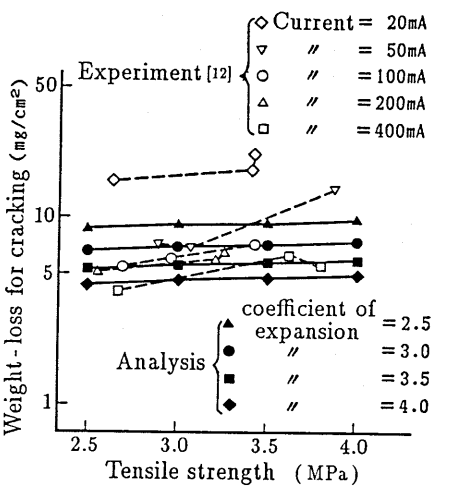

Fig.13 Tensile strength vs. weight loss for cracking

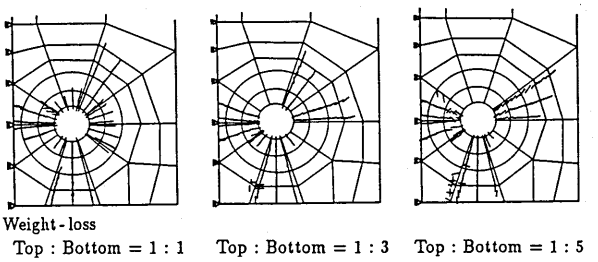

Fig.14 Influence of non-uniform corrosion

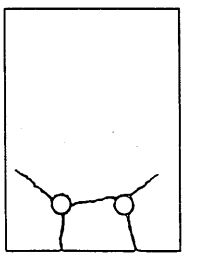

Fig.15 Crack situation in experiment [14][15]

5. CONCLUSIONS

In this study, a model for expansive behavior by the corrosion of reinforcement was proposed and tested of its applicability by comparing its results of analysis with experimental result. Results were summarized as follows;

(1) Expansive behavior by corrosion was well represented by the method in which corrosion products were considered to be a thin layer and arranged by one layer element and the expansion was provided by volumetric strain.
(2) As the result of analysis made using this model, the relation between the weight-loss of corrosion for cracking and the coefficient of expansion of corrosion products were obtained. Expansive pressure at that time was found to be 9-10 MPa.
(3) Elastic modulus and Poisson's ratio of corrosion products were found not to influence for cracking by the corrosion of reinforcement.
(4) It was found by the analysis also that the cover of reinforcement influenced for cracking by the corrosion greatly, but that the tensile strength of concrete did little.
(5) The situation of cracks could rather be understood well by considering the difference in the extent of corrosion between the top and the bottom of reinforcement.

References

[1] A.P.Crane : Corrosion of Reinforcement in Concrete Construction, Ellis Horwood Limited, 1983.
[2] K.Okada, W.Koyanagi and T.Miyagawa : Chloride Corrosion of Reinforcing Steel in Cracked Concrete, Proc. of JSCE, No.281, pp.75-87, 1979.
[3] T.Uomoto, K.Tsuji and T.Kakizawa : Mechanism of Deterioration of Concrete Stractures Caused by Corrosion of Reinforcing Bars, JCI 6th Conference, pp.173-176, 1984.
[4] M.Tsunomoto, Y.Kajikawa and Y.Tachibana : Elasto-Plastic Analysis of Expansive Behavior by Corrosion of Reinforcement, Proc. of the Annual Conference of the JSCE, 1987.
[5] Y.Konishi, H.Seki, K.Matsui and M.Matsushima : FEM Analysis of Cracking of Concrete due to Expansion by Rebar Corrosion, Proc. of the Annual Conference of the JSCE, 1987.
[6] H.Seki : Mechanism of Longitudinal Crack due to Corrosion of Reinforcing Bars, Cement & Concrete, No.458, pp.20-27, 1985.
[7] Y.Yamada and Y.Ezawa : Joint Elements and theis Application to the Finite Element Analysis, Monthly Journal of Institute of Industrial Science, University of Tokyo, Vol.31, No.6, pp.519-524, 1979.
[8] D.R.J.Owen and E.Hinton : Finite Elements in Plasticity, Pineridge Press Limited, 1980.
[9] W.F.Chen : Plasticity in Reinforced Concrete, McGraw-Hill, 1982.
[10] H.Kupfer, H.K.Hilsdorf and H.Rüsch : Behavior of Concrete under Biaxial Stresses, ACI Journal, Vol.66, pp.656-666, 1969.
[11] Y.Aoyagi and K.Yamada : Strength and Deformation Characteristics of Reinforced Concrete Shell Elements Subjected to In-Plane Forces, Proc. of JSCE, No.331, pp.167-180, 1983.
[12] M.Morikawa, H.Seki and Y.Okumura : Basic Study on Cracking of Concrete due to Expansion by Rebar Corrosion, Proc. of JSCE, No.378, pp.97-105, 1987.
[13] Y.Yoshioka and T.Yonezawa : Basic Study about mechanical Characteristics of Reinforcement's Corrosion, Proc. of the Annual Conferance of the JSCE,1982.
[14] K.Tamori, K.Maruyama, M.Odagawa and C.Hashimoto : Crack Behavior of Reinforced Concrete Members Due to Corrosion of Reinforcing Bars, Proc. of the JCI, Vol.10, pp.505-510, 1988.
[15] Y.Tachibana, Y.kajikawa and M.Kawamura : The Behaviour of RC Beams Damaged by Corrosion of Reinforcement, Proc. of JSCE, No.402, pp.105-114, 1989.